

Asymptotic Characterisation of Regularised Zero-Forcing Receiver for Imperfect and Correlated Massive MIMO Systems with Optimal Power Allocation

Ayed M. Alrashdi

Abstract—In this paper, we present asymptotic high dimensional analysis of the regularised zero-forcing (RZF) receiver in terms of its mean squared error (MSE) and bit error rate (BER) when used for the recovery of binary phase shift keying (BPSK) modulated signals in a massive multiple-input multiple-output (MIMO) communication system. We assume that the channel matrix is spatially correlated and not perfectly known. We use the linear minimum mean squared error (LMMSE) method to estimate the channel matrix. The asymptotic approximations of the MSE and BER enable us to solve various practical optimisation problems. Under MSE/BER minimisation, we derive 1) the optimal regularisation factor for RZF; 2) the optimal power allocation scheme. Numerical simulations show a close match to the derived asymptotic results even for a few dozens of the problem dimensions.

Index Terms—Regularisation, spatial correlation, channel estimation, power allocation, performance analysis, Gaussian min-max theorem.

I. INTRODUCTION

SINCE the early works of [1], [2], massive multiple-input multiple-output (MIMO) research has been thriving.

The idea of massive MIMO is to use a very large number of antennas at the base station which offers the desired spatial multiplexing and can reduce the transmitted power [2]. Therefore, it has been considered a promising vital technology to achieve the high spectral/energy efficiencies and high data rates required by the fifth generation (5G) and next wireless communication generations [3].

Channel state information (CSI) plays an important role in attaining the significant benefits of massive MIMO systems, and accurately recovering the transmitted symbols [3]. It is well known that perfect knowledge of CSI is an ideal scenario that is impossible to obtain. However, in practice, only imperfect or partial CSI can be acquired through a process called channel estimation or training. Training refers to the process of sending a known sequence of pilot symbols which can be directly incorporated in the process of estimating the CSI. After this step, the receiver employs the estimated CSI to detect the corresponding transmitted data symbols.

The overall system performance can be improved by optimising the power allocation between the transmitted pilot and

data symbols. Power optimisation problems in MIMO systems have been proposed based on different performance metrics. In [4], [5], the authors derived a power allocation scheme based on minimising the mean squared error (MSE), while minimising the the bit error rate (BER) and symbol error rate (SER) was considered in [6]–[8]. Training optimisation based on maximising the channel capacity was addressed in [9]–[11]. In addition, the authors in [12]–[14] provided power allocation strategies based on maximising the sum rates. Training optimisation problems are considered in a wide range of systems including traditional MIMO systems [11], single-cell massive MIMO systems [15] and multi-cell multi-user MIMO networks [13], [16], [17]. The list of above references is not inclusive, since power allocation optimisation research has very rich literature. However, we cited the most related works to this paper.

The power allocation in the aforementioned papers was investigated essentially for uncorrelated channel models. However, in practice, wireless communication systems, including massive MIMO systems, are generally spatially correlated [18]. The power allocation optimisation problem was developed for correlated channels to maximise the sum rates [19], [20], or the spectral efficiency [15], [21]. To the best of our knowledge, power optimisation problems based on MSE or BER minimisation that involve spatial correlation models in massive MIMO systems are largely unexplored.

In this paper, we propose the use of the regularised zero-forcing (RZF) as a low complexity receiver for a spatially correlated massive MIMO system. We derive novel sharp asymptotic approximations of its MSE and BER performance using binary phase shift keying (BPSK) signaling for simplicity. Then, these approximations are used to derive an optimal power allocation scheme between pilot and data symbols. The main technical tool used in our analysis is the recently developed convex Gaussian min-max Theorem (cGMT) [22], [23]. The cGMT framework has been used to analyse the error performance of many regression problems under independent and identically distributed (i.i.d.) assumption on the entries of the channel matrix [22]–[28]. For correlated channel matrices, the cGMT was recently used in [29], [30] to characterise the performance of the Box-relaxation and the LASSO detectors, respectively. However, these references assume the ideal case of perfect knowledge of the CSI which is impossible to obtain in practice, while this work deals with the more difficult and

The author is with the Department of Electrical Engineering, College of Engineering, University of Ha'il, P.O. Box 2440, Ha'il, 81441, Saudi Arabia (e-mail: am.alrashdi@uoh.edu.sa).

common in practice scenario of imperfect CSI.

A. Organisation

The remainder of this paper is structured as follows. Section II describes the system model and the considered RZF receiver. The main asymptotic analysis results are presented in Section III. Section IV presents the numerical simulations used to verify the high accuracy of our results. In addition, Section V illustrates the optimal power allocation scheme derived in this paper. The paper is then concluded in Section VI. Finally, the approach of the proof of the main results is given in Appendix A.

B. Notations

Bold face lower case letters (e.g., \mathbf{x}) represent a column vector while x_i is its i^{th} entry and $\|\mathbf{x}\|$ represents its ℓ_2 -norm. Matrices are denoted by upper case letters such as \mathbf{X} , with \mathbf{I}_n being the $n \times n$ identity matrix, while $\mathbf{0}_{m \times n}$ is the all-zeros matrix of size $m \times n$. The (i, j) entry of matrix \mathbf{X} is denoted as $[\mathbf{X}]_{ij}$. $\text{tr}(\cdot)$, $(\cdot)^T$, and $(\cdot)^{-1}$ are the trace, transpose and inverse operators, respectively. $\mathbf{X}^{1/2}$ represents the square root of matrix \mathbf{X} such that $\mathbf{X} = \mathbf{X}^{1/2} \mathbf{X}^{T/2}$. We use the standard notations $\mathbb{E}[\cdot]$, and $\mathbb{P}[\cdot]$ to denote the expectation of a random variable, and probability of an event, respectively. The notation $\mathbf{q} \sim \mathcal{N}(\mathbf{0}, \mathbf{R}_q)$ is used to denote that the random vector \mathbf{q} is normally distributed with $\mathbf{0}$ mean and covariance matrix $\mathbf{R}_q = \mathbb{E}[\mathbf{q}\mathbf{q}^T]$, where $\mathbf{0}$ represent the all-zeros vector. We write “ \xrightarrow{P} ” to denote convergence in probability as $n \rightarrow \infty$. The notation $f(t) = \mathcal{O}(g(t))$ means $\left| \frac{f(t)}{g(t)} \right|$ is bounded as $t \rightarrow \infty$. Finally, $Q(x) = \frac{1}{\sqrt{2\pi}} \int_x^\infty e^{-u^2/2} du$ is the Q -function associated with the standard normal density.

II. SYSTEM MODEL AND SIGNAL DETECTION

We consider a flat block-fading massive MIMO system with n transmitters (Tx) and m receivers (Rx). The transmission consists of T symbols that occur in a time interval within which the channel is assumed to be constant. A number T_t pilot symbols (for channel estimation) occupy the first part of the transmission interval with power, ρ_t . The remaining part is reserved for transmitting $T_d = T - T_t$ data symbols with power, ρ_d . It implies from conservation of time and energy that:

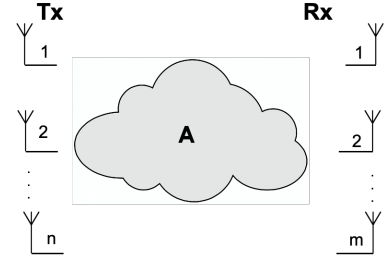
$$\rho_t T_t + \rho_d T_d = \rho T, \quad (1)$$

where ρ is the expected average power. Alternatively, we have $\rho_d T_d = \alpha \rho T$, where $\alpha \in (0, 1)$ is the ratio of the power allocated to the data, then $\rho_t T_t = (1 - \alpha) \rho T$ is the energy of the pilots. Fig. 1 illustrates the considered system model.

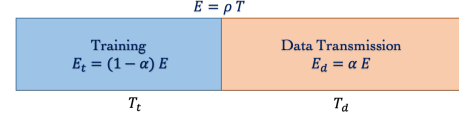
The received signal model for the *data* transmission phase is given by

$$\mathbf{y} = \sqrt{\frac{\rho_d}{n}} \mathbf{A} \mathbf{x}_0 + \mathbf{w}, \quad (2)$$

where the following model-assumptions hold, except if otherwise stated:



(a) A massive MIMO system.



(b) Pilot-based transmission.

Fig. 1: System model.

- The MIMO channel matrix is given by [19]

$$\mathbf{A} = \mathbf{R}^{1/2} \mathbf{H}. \quad (3)$$

This matrix model is referred to as the receive-correlated Kronecker model [31]. This implies that \mathbf{A} has n i.i.d. columns, each with zero mean and covariance matrix \mathbf{R} .

- $\mathbf{H} \in \mathbb{R}^{m \times n}$ is a random matrix which has i.i.d. standard Gaussian entries (with zero mean and unit variance).
- $\mathbf{R} \in \mathbb{R}^{m \times m}$ is a positive semi-definite Hermitian matrix, satisfying¹ $\frac{1}{m} \text{tr}(\mathbf{R}) = \mathcal{O}(1)$. It captures the spatial correlation between the receive antennas and hence termed the receive-correlation matrix.
- $\mathbf{w} \in \mathbb{R}^m$ is the noise vector with i.i.d. standard Gaussian entries, i.e., $\mathbf{w} \sim \mathcal{N}(\mathbf{0}, \mathbf{I}_m)$.
- $\mathbf{x}_0 \in \mathbb{R}^n$ is the signal to be recovered, which is assumed to be a binary phase shift keying (BPSK) signal, i.e., $\mathbf{x}_0 \in \{\pm 1\}^n$.

A. Channel Matrix Estimation

In this paper, we consider the linear minimum mean squared error (LMMSE) estimate $\hat{\mathbf{A}}$ of the channel matrix \mathbf{A} , which is given by [32]

$$\hat{\mathbf{A}} = \sqrt{\frac{n}{\rho_t}} \mathbf{R} \left(\mathbf{R} + \frac{n}{T_t \rho_t} \mathbf{I}_m \right)^{-1} \mathbf{Y}_t \mathbf{X}_t^T, \quad (4)$$

where $\mathbf{Y}_t = \sqrt{\frac{\rho_t}{n}} \mathbf{A} \mathbf{X}_t + \mathbf{W}_t \in \mathbb{R}^{m \times T_t}$ is the received signal corresponding to the *training* phase, $\mathbf{X}_t \in \mathbb{R}^{n \times T_t}$ is the matrix of transmitted orthogonal pilot symbols with $T_t \geq n$, and $\mathbf{W}_t \in \mathbb{R}^{m \times T_t}$ is an additive white Gaussian noise (AWGN) matrix with $\mathbb{E}[\mathbf{W}_t \mathbf{W}_t^T] = T_t \mathbf{I}_m$.

According to [32], [33], the k^{th} column (for all $k \leq n$) of $\hat{\mathbf{A}}$ is distributed as $\mathcal{N}(\mathbf{0}, \mathbf{R}_{\hat{\mathbf{A}}})$ with a covariance matrix $\mathbf{R}_{\hat{\mathbf{A}}}$ that is given by

$$\mathbf{R}_{\hat{\mathbf{A}}} = \mathbf{R} \left(\mathbf{R} + \frac{n}{T_t \rho_t} \mathbf{I}_m \right)^{-1} \mathbf{R}. \quad (5)$$

¹We assume this for analytical simplicity.

Note that the pilots energy $T_t \rho_t$ controls the quality of the estimation. In fact, as $T_t \rho_t \rightarrow \infty$, $\hat{\mathbf{A}} \rightarrow \mathbf{A}$ which corresponds to the perfect CSI case.

By invoking the orthogonality principle of the LMMSE estimator, it can be shown that the k^{th} column of the *estimation error matrix* $\mathbf{\Delta} := \hat{\mathbf{A}} - \mathbf{A}$ follows the distribution $\mathcal{N}(\mathbf{0}, \mathbf{R}_{\Delta})$ with the following covariance matrix [32]:

$$\mathbf{R}_{\Delta} = \mathbf{R} - \mathbf{R}_{\hat{\mathbf{A}}}.$$

From the orthogonality principle of the LMMSE as well, one can show that $\hat{\mathbf{A}}$ and $\mathbf{\Delta}$ are uncorrelated, but both of them follow a Gaussian distribution, hence they are statistically independent.²

B. Signal Detection: RZF Receiver

In this work, we consider the regularised zero-forcing (RZF) receiver that solves the following optimisation

$$\hat{\mathbf{x}} := \arg \min_{\mathbf{x}} \|\mathbf{y} - \sqrt{\frac{\rho_d}{n}} \hat{\mathbf{A}} \mathbf{x}\|^2 + \rho_d \lambda \|\mathbf{x}\|^2, \quad (6)$$

where $\lambda \geq 0$ is the regularisation factor. For this RZF receiver, $\hat{\mathbf{x}}$ admits the following closed-form solution:

$$\hat{\mathbf{x}} = \left(\tilde{\mathbf{A}}^T \tilde{\mathbf{A}} + \rho_d \lambda \mathbf{I}_n \right)^{-1} \tilde{\mathbf{A}}^T \mathbf{y}, \quad (7)$$

with $\tilde{\mathbf{A}} := \sqrt{\frac{\rho_d}{n}} \hat{\mathbf{A}}$. For this receiver, the detection is performed as follows

$$\mathbf{x}^* := \text{sign}(\hat{\mathbf{x}}), \quad (8)$$

where $\text{sign}(\cdot)$ is the sign function which operates element-wise on vector inputs.

C. Figures of Merit

To evaluate the performance of the RZF receiver, we consider the following performance metrics:

1) *Mean Squared Error (MSE)*: This measures the performance of the estimation step of the receiver (the first step in (6)) and is defined as:

$$\text{MSE}_n := \frac{1}{n} \|\mathbf{x}_0 - \hat{\mathbf{x}}\|^2. \quad (9)$$

2) *Bit Error Rate (BER)*: This metric is used to evaluate the performance of the second step of the receiver, i.e., the detection step in (8). It is defined as

$$\text{BER}_n := \frac{1}{n} \sum_{i=1}^n \mathbf{1}_{\{x_i^* \neq x_{0,i}\}}, \quad (10)$$

where $\mathbf{1}_{\{\cdot\}}$ is the indicator function.

In relation to the BER is the *probability of error*, P_e , which is defined as the expected value of the BER averaged over the noise, the channel and the constellation. Formally,

$$P_e := \mathbb{E}[\text{BER}_n] = \frac{1}{n} \sum_{i=1}^n \mathbb{P}[\{x_i^* \neq x_{0,i}\}]. \quad (11)$$

²This independence notion is needed in deriving the cGMT results. Since, in (28a), $\xi(\mathbf{a}, \mathbf{b})$ should be independent of \mathbf{A} , then by expressing \mathbf{A} as $\mathbf{A} = \hat{\mathbf{A}} + \mathbf{\Delta}$, one can ensure that.

III. MAIN RESULTS

In this section, we provide our main results on the asymptotic characterisation of the RZF receiver in terms of its MSE and BER.

A. Technical Assumptions

First, we need to state some technical assumptions that are required for our analytical analysis.

Assumption (1): We assume that the problem dimensions m and n are growing large to infinity with a fixed ratio, i.e.,

$$m \rightarrow \infty, n \rightarrow \infty, \frac{m}{n} \rightarrow \zeta,$$

for some fixed constant $\zeta > 0$.

Assumption (2): We assume that the normalised coherence time, normalised number of pilot symbols and normalised number data symbols are fixed and given as

$$\begin{aligned} \frac{T}{n} &\rightarrow \tau \in (1, \infty), \\ \frac{T_t}{n} &\rightarrow \tau_t \in [1, \infty), \end{aligned}$$

and

$$\frac{T_d}{n} \rightarrow \tau_d,$$

respectively.

Note that under Assumption (2), the covariance matrix of $\hat{\mathbf{A}}$ becomes

$$\mathbf{R}_{\hat{\mathbf{A}}} = \mathbf{R} \left(\mathbf{R} + \frac{1}{\tau_t \rho_t} \mathbf{I}_m \right)^{-1} \mathbf{R},$$

and the time/energy conservation equation in (1) becomes

$$\rho_t \tau_t + \rho_d \tau_d = \rho \tau. \quad (12)$$

Finally, define the spectral decomposition of $\mathbf{R}_{\hat{\mathbf{A}}}$ as

$$\mathbf{R}_{\hat{\mathbf{A}}} = \mathbf{U} \mathbf{\Gamma} \mathbf{U}^T,$$

where $\mathbf{U} \in \mathbb{R}^{m \times m}$ is an orthonormal matrix, and $\mathbf{\Gamma} \in \mathbb{R}^{m \times m}$ is a diagonal matrix with the eigenvalues of $\mathbf{R}_{\hat{\mathbf{A}}}$ on its main diagonal.

B. RZF Receiver Performance Characterisation

In this subsection, we precisely characterise the high dimensional performance of the RZF receiver. We begin by stating the MSE analysis as given in the next theorem.

Theorem 1 (MSE of RZF). Let $\hat{\mathbf{x}}$ be a minimiser of the RZF problem in (6) for some fixed but unknown BPSK signal \mathbf{x}_0 , then for any fixed $\lambda > 0, \zeta > 0$, and under Assumptions (1) and (2), it holds that

$$|\text{MSE}_n - \nu_*| \xrightarrow{P} 0. \quad (13)$$

where ν_* is the unique solution to the following scalar minimax optimisation problem:

$$\begin{aligned} \min_{\nu > 0} \max_{\mu > 0} \mathcal{F}(\nu, \mu) &:= \frac{1}{2n} \sum_{j=1}^m \frac{\gamma_j \rho_d \nu + \rho_d [\mathbf{R}_{\Delta}]_{jj} + 1}{\frac{1}{2} + \frac{\rho_d \gamma_j}{\mu}} \\ &+ \lambda \rho_d (\nu + 1) - \frac{\nu \mu}{2} - \frac{2 \lambda^2 \rho_d^2}{\mu}, \end{aligned} \quad (14)$$

and γ_j is the j^{th} eigenvalue of $\mathbf{R}_{\hat{A}}$.

Proof. The proof of this theorem is given in Appendix A. \square

Remark 1. From the first order optimality conditions, i.e.,

$$\nabla_{(\nu, \mu)} \mathcal{F}(\nu, \mu) = \mathbf{0}, \quad (15)$$

the solutions (ν_*, μ_*) can be efficiently found as:

$$\nu_* = \frac{\frac{1}{n} \sum_{j=1}^m \frac{\rho_d \gamma_j (\rho_d [\mathbf{R}_{\Delta}]_{jj} + 1)}{(\frac{\mu_*}{2} + \rho_d \gamma_j)^2} + \frac{4\lambda^2 \rho_d^2}{\mu_*^2}}{1 - \frac{1}{n} \sum_{j=1}^m \frac{\rho_d \gamma_j^2}{(\frac{\mu_*}{2} + \rho_d \gamma_j)^2}}, \quad (16)$$

and μ_* is the solution to the following fixed-point equation:

$$\mu_* = \frac{1}{n} \sum_{j=1}^m \frac{\mu_* \rho_d \gamma_j}{\frac{\mu_*}{2} + \rho_d \gamma_j} + 2\lambda \rho_d. \quad (17)$$

Remark 2. For $\mathbf{R} = \mathbf{I}$, (i.e., no correlation, $\gamma_i = 1 \forall i$) and perfect CSI ($\Delta = \mathbf{0}_{m \times n}$), we recover the well-known MSE formula of the Zero-Forcing (ZF) receiver (i.e., when $\lambda = 0$):

$$\nu_* = \frac{1}{(\zeta - 1)\rho_d}. \quad (18)$$

Note that the MSE result of Theorem 1 holds for \mathbf{x}_0 drawn from any distribution with zero mean and unit variance and not necessarily from a BPSK constellation. However, for BPSK signals, the BER of the RZF receiver is given in the next Theorem.

Theorem 2 (BER of RZF). For $\nu > 0$, and $\mu > 0$, define

$$S_\gamma(\nu, \mu) := \frac{1}{n} \sum_{j=1}^m \frac{\rho_d \gamma_j^2 \nu + \rho_d \gamma_j (\rho_d [\mathbf{R}_{\Delta}]_{jj} + 1)}{(\frac{1}{2} + \frac{\rho_d \gamma_j}{\mu})^2}. \quad (19)$$

Then, under the same settings of Theorem 1, it holds that

$$\left| \text{BER}_n - Q \left(\sqrt{\frac{4\lambda^2 \rho_d (1 - \nu_*) + S_\gamma(\nu_*, \mu_*)}{\nu_* S_\gamma(\nu_*, \mu_*)}} \right) \right| \xrightarrow{P} 0. \quad (20)$$

Proof. The proof is postponed to Appendix A. \square

Remark 3 (Probability of error). Recall that $P_e = \mathbb{E}[\text{BER}]$, then using [23, Theorem II.1], we can show that P_e converges to the same asymptotic value as the BER. This means that

$$\left| P_e - Q \left(\sqrt{\frac{4\lambda^2 \rho_d (1 - \nu_*) + S_\gamma(\nu_*, \mu_*)}{\nu_* S_\gamma(\nu_*, \mu_*)}} \right) \right| \xrightarrow{P} 0. \quad (21)$$

Corollary 1 (Optimal regulariser). The optimal regularisation factor that minimises the MSE or BER is given as

$$\lambda_* = \frac{1}{\rho_d} + \frac{1}{m} \text{tr}(\mathbf{R}_{\Delta}). \quad (22)$$

Proof. Note that the MSE expression depends on λ through ν_* only. Hence, the above result can be proven by taking the derivative of ν_* with respect to λ . In addition, λ_* turned out to be optimal in the BER sense as well. This can be shown by taking the derivative of (20) with respect to λ . \square

Remark 4. Under perfect CSI ($\Delta = \mathbf{0}_{m \times n}$), Corollary 1 simplifies to the well-known formula: $\lambda_* = \frac{1}{\rho_d}$, independent of the correlation matrix \mathbf{R} , which was previously shown in

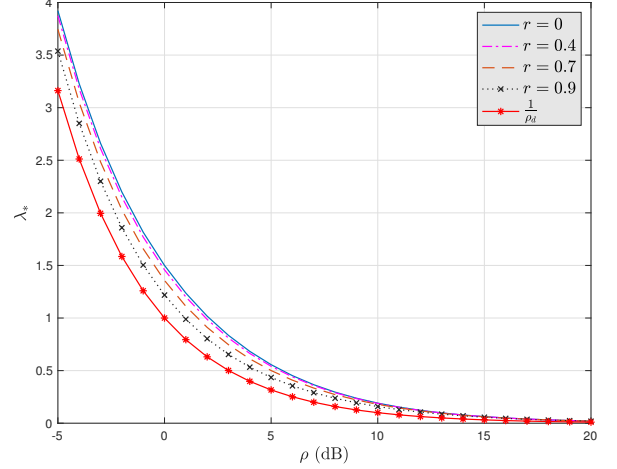


Fig. 2: Optimal regulariser λ_* v.s. ρ for different correlation coefficients r , with $\zeta = 1.5, n = 500, \alpha = 0.5, T = 1000, T_t = n$.

[19], [34] for other optimality metrics such as maximising the sum rate or SINR, etc. Here, our optimality metrics are MSE and BER which were not considered for the correlated channel model before. As mentioned in [34], for large n , the RZF receiver is equivalent to the MMSE. For uncorrelated channels ($\mathbf{R} = \mathbf{I}_m$, and $\mathbf{R}_{\Delta} = \sigma_{\Delta}^2 \mathbf{I}_m$), it was proven in [7] that $\lambda_* = \frac{1}{\rho_d} + \sigma_{\Delta}^2$, which is consistent with (22).

In Fig. 2, we use the exponential correlation model for \mathbf{R} which is defined as [35]

$$\mathbf{R}(r) = \left[r^{|i-j|} \right]_{i,j=1,2,\dots,m}, \quad r \in [0, 1), \quad (23)$$

to show the effect of increasing the correlation on the optimal regularisation factor and compare it with the perfect CSI case, i.e., $\lambda_* = \frac{1}{\rho_d}$. As we can see, for the imperfect CSI scenario, more regularisation is needed due to the channel estimation errors. Furthermore, we observe that as r increases, less regularisation is needed.

IV. NUMERICAL RESULTS

To validate our theoretical predictions of the MSE and BER as given by Theorem 1 and Theorem 2, we consider the exponential model given earlier in (23). Fig. 3 shows the MSE/BER curves v.s. the regularisation factor λ . For the Monte-Carlo (MC) simulations, we used $\zeta = 1.5, n = 400, r = 0.4, \alpha = 0.5, T = 1000, T_t = n$, and $\rho = 10$ dB, and the data are averaged over 500 independent Monte-Carlo trials. We can see that from both figures, there is an optimal value of the regulariser λ_* that minimises the MSE/BER. This optimal value is the same for MSE or BER as we can see from the figures.

In addition, we plotted in Fig. 4, and Fig. 5 the MSE/BER performance of the RZF receiver versus the total average power ρ and for different correlation coefficient r values. We used the same parameters values as in the previous experiment. These figures again show the great match between our analytical expressions and the MC simulations.

Finally, in Fig. 6, we compare the BER performance of the RZF receiver to the conventional zero-forcing (ZF) receiver (i.e., $\lambda = 0$) that is widely used in wireless communications literature. From this figure, it can be seen that the RZF receiver clearly outperforms the ZF.

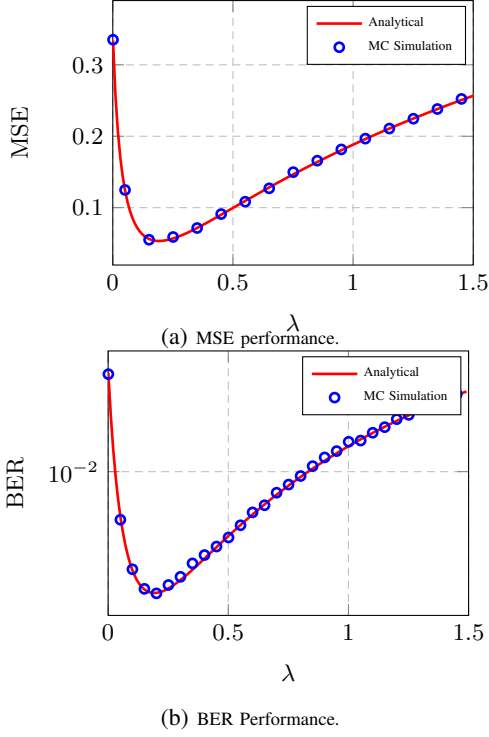


Fig. 3: Performance of RZF receiver v.s. the regulariser λ . We used $\zeta = 1.5$, $n = 400$, $r = 0.4$, $T_t = n$, $T = 1000$, $\alpha = 0.5$, $\rho = 10$ dB.

V. POWER ALLOCATION OPTIMISATION

In this section, we will use the previous asymptotic approximations of the MSE and BER to find the optimum power allocation between pilot and data symbols to asymptotically

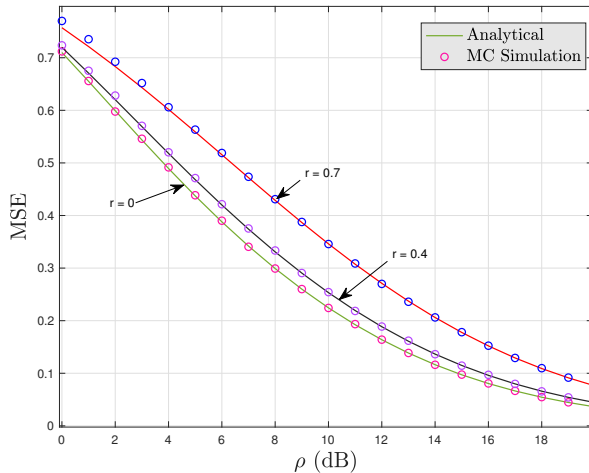


Fig. 4: MSE performance of RZF receiver v.s. ρ for different correlation coefficients r , with $\zeta = 1.5$, $n = 500$, $\alpha = 0.5$, $T = 1000$, $T_t = n$.

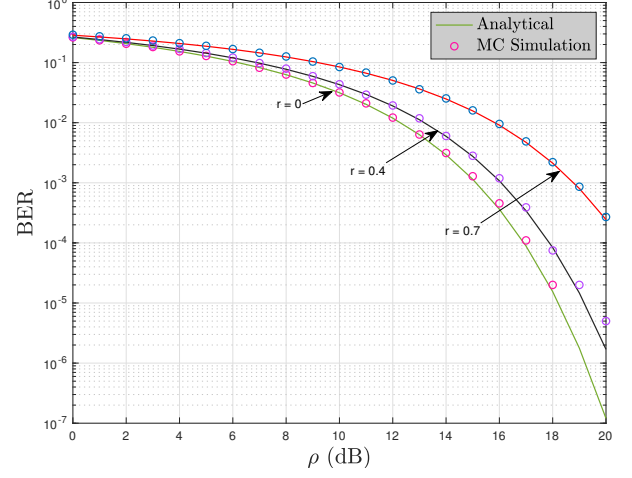


Fig. 5: BER performance of RZF receiver v.s. ρ for different correlation coefficients r , with $\zeta = 1.5$, $n = 500$, $\alpha = 0.5$, $T = 1000$, $T_t = n$.

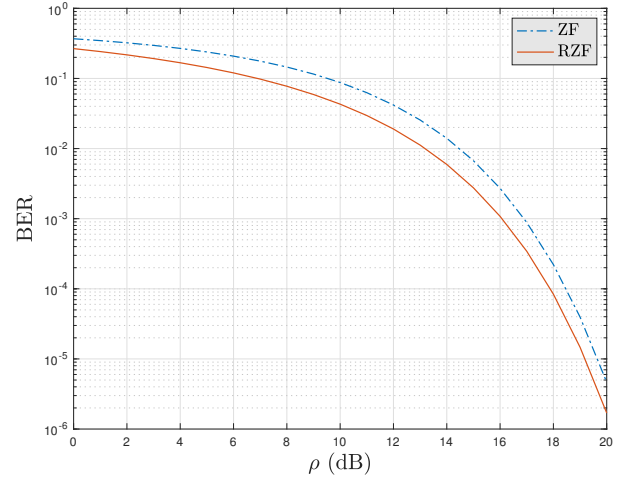


Fig. 6: Comparison between BER performance of ZF and RZF receivers. We used the same parameter values as in Fig. 5, but with $r = 0.4$.

minimise the MSE or BER. For fixed τ_t and τ , the power allocation optimisation problem can be cast as

$$\begin{aligned} & \min_{\rho_t, \rho_d} \text{MSE} \\ & \text{subject to: } \rho_t \tau_t + \rho_d (\tau - \tau_t) = \rho \tau, \\ & \rho_t = (1 - \alpha) \rho \tau, \rho_d = \alpha \rho \tau, 0 < \alpha < 1. \end{aligned}$$

It can be shown that the above optimisation problem boils down to only optimising the data power ratio α , i.e.,

$$\alpha_*^{\text{MSE}} = \arg \min_{0 < \alpha < 1} \text{MSE}(\lambda_*), \quad (24)$$

where $\text{MSE}(\lambda_*)$ is the asymptotic MSE expression in (13) while using the optimal value of the regulariser λ_* there. Similarly, we have

$$\alpha_*^{\text{BER}} = \arg \min_{0 < \alpha < 1} \text{BER}(\lambda_*), \quad (25)$$

where $\text{BER}(\lambda_*)$ is the asymptotic BER expression in (20), but with optimal λ_* . However, based on (20), since minimising the Q -function amounts to maximising its argument, we have

$$\alpha_*^{\text{BER}} = \arg \max_{0 < \alpha < 1} \mu_*. \quad (26)$$

For this RZF receiver, finding α_*^{MSE} or α_*^{BER} in a closed form seems to be a difficult task, but by using a bisection method we can numerically find the optimal power allocation as shown in Fig. 7 for different values of the correlation coefficient r . In [7], for the uncorrelated channel $\mathbf{R} = \mathbf{I}_m$, it has been shown that $\bar{\alpha}_*^{\text{MSE}} = \bar{\alpha}_*^{\text{BER}} = \bar{\alpha}_*$, where $\bar{\alpha}_*$ has the following closed-form expression (see [7, eq. (36)]):

$$\bar{\alpha}_* = \begin{cases} \vartheta - \sqrt{\vartheta(\vartheta - 1)}, & \text{if } \tau_d > 1, \\ \frac{1}{2}, & \text{if } \tau_d = 1, \\ \vartheta + \sqrt{\vartheta(\vartheta - 1)} & \text{if } \tau_d < 1, \end{cases} \quad (27)$$

where $\vartheta = \frac{1+\rho\tau}{\rho\tau(1-\frac{1}{\tau_d})}$. From Fig. 7, we can see that even for the correlated case, we still have that $\alpha_*^{\text{MSE}} = \alpha_*^{\text{BER}}$ which indicates that optimising the MSE is equivalent to optimising the BER asymptotically. Furthermore, from this figure we can see that $\bar{\alpha}_*$ is a quite good approximation of α_* for $r \in [0, 0.9]$. This suggests that we can use the optimal $\bar{\alpha}_*$ from the uncorrelated channel model for the correlated channel case with negligible effect on the performance. Similar observations were found in [20].

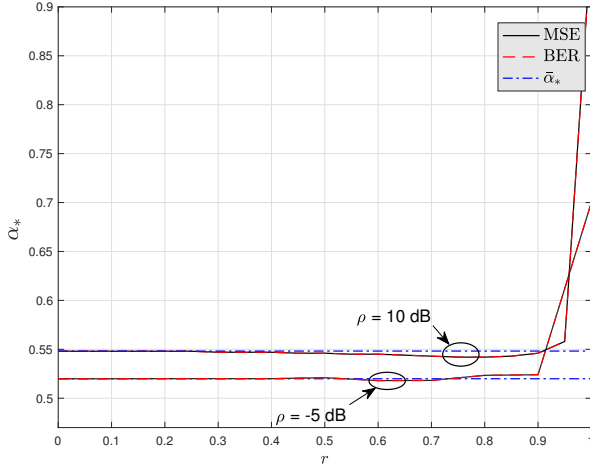


Fig. 7: Optimal data power ratio α_* v.s. correlation coefficient r , with $\zeta = 1.5$, $n = 400$, $T = 1000$, $T_t = n$.

VI. CONCLUSION

This work sharply characterises the asymptotic behaviour of the RZF receiver under the presence of correlation and uncertainties (in the form of estimation errors) in the channel matrix. Particularly, we derived asymptotic expressions of the MSE and BER of the RZF. We then considered a concrete application of our theoretical results to a BPSK modulated massive MIMO wireless communication system, and optimise

its performance by optimally allocating power between pilot and data symbols. The results also enabled us to set the regularisation factor in an optimal way which was shown to further improves the performance. Numerical results showed great agreement to the derived theoretical expressions even when the dimensions are not very large.

Possible future extensions of this work include: studying more involved modulation schemes (such as PAM, QAM, and PSK), and analyzing advanced receivers such as the RZF with a box-constraint. Another interesting future work is to consider the performance of double-sided correlated massive MIMO systems and study their optimal power allocation.

ACKNOWLEDGMENT

The work of Ayed M. Alrashdi is supported by the University of Ha'il, Saudi Arabia.

APPENDIX A APPROACH OF THE PROOF

In this section, we prove the main results of the *RZF receiver*. We first introduce the main tool used in the analysis, i.e., the cGMT.

A. cGMT Framework

The proof is based on the cGMT framework [22]. Here, we recall the statement of the theorem, and we refer the reader to [22], [23] for the complete technical details. Consider the following two min-max problems, which we refer to, respectively, as the Primal Optimisation (PO) and Auxiliary Optimisation (AO):

$$(\text{PO}) \quad \Psi^{(n)}(\mathbf{C}) := \min_{\mathbf{a} \in \mathcal{K}_a} \max_{\mathbf{b} \in \mathcal{K}_b} \mathbf{b}^T \mathbf{C} \mathbf{a} + \xi(\mathbf{a}, \mathbf{b}), \quad (28a)$$

$$(\text{AO}) \quad \psi^{(n)}(\mathbf{g}_1, \mathbf{g}_2) := \min_{\mathbf{a} \in \mathcal{K}_a} \max_{\mathbf{b} \in \mathcal{K}_b} \|\mathbf{a}\| \mathbf{g}_1^T \mathbf{b} - \|\mathbf{b}\| \mathbf{g}_2^T \mathbf{a} + \xi(\mathbf{a}, \mathbf{b}), \quad (28b)$$

where $\mathbf{C} \in \mathbb{R}^{\tilde{m} \times \tilde{n}}$, $\mathbf{g}_1 \in \mathbb{R}^{\tilde{m}}$, $\mathbf{g}_2 \in \mathbb{R}^{\tilde{n}}$, $\mathcal{K}_a \subset \mathbb{R}^{\tilde{n}}$, $\mathcal{K}_b \subset \mathbb{R}^{\tilde{m}}$ and $\xi: \mathbb{R}^{\tilde{n}} \times \mathbb{R}^{\tilde{m}} \mapsto \mathbb{R}$. Moreover, the function ξ is assumed to be independent of the matrix \mathbf{C} . Denote by $\mathbf{a}_\Psi := \mathbf{a}_\Psi(\mathbf{C})$, and $\mathbf{a}_\psi := \mathbf{a}_\psi(\mathbf{g}_1, \mathbf{g}_2)$ any optimal minimisers of (28a) and (28b), respectively. Further let $\mathcal{K}_a, \mathcal{K}_b$ be convex and compact sets, $\xi(\mathbf{a}, \mathbf{b})$ is convex-concave continuous on $\mathcal{K}_a \times \mathcal{K}_b$, and \mathbf{C}, \mathbf{g}_1 and \mathbf{g}_2 all have i.i.d. standard normal entries. Then, the cGMT framework relates the optimiser \mathbf{a}_Ψ of the PO with the optimal value of the AO as summarised in the following theorem.

Theorem 3 (cGMT, [22]). *Let \mathcal{K} be any arbitrary open subset of \mathcal{K}_a , and $\mathcal{K}^c = \mathcal{K}_a \setminus \mathcal{K}$. Denote $\psi_{\mathcal{K}^c}^{(n)}(\mathbf{g}_1, \mathbf{g}_2)$ the optimal cost of the optimisation in (28b), when the minimisation over \mathbf{a} is constrained over $\mathbf{a} \in \mathcal{K}^c$. Suppose that there exist constants β and $\delta > 0$ such that in the limit as $\tilde{n} \rightarrow +\infty$, it holds with probability approaching one: (i) $\psi^{(n)}(\mathbf{g}_1, \mathbf{g}_2) \leq \beta + \delta$, and, (ii) $\psi_{\mathcal{K}^c}^{(n)}(\mathbf{g}_1, \mathbf{g}_2) \geq \beta + 2\delta$. Then,*

$$\lim_{\tilde{n} \rightarrow \infty} \mathbb{P}[\mathbf{a}_\Psi \in \mathcal{K}] = 1. \quad (29)$$

After introducing the cGMT, we are now in a position to outline the proof of Theorem 1 and Theorem 2. The steps of the proof are given in the next subsections.

B. Deriving the Minimax Optimisation

For convenience, we consider the *error vector* $\mathbf{e} := \mathbf{x} - \mathbf{x}_0$, then the problem in (6) can be reformulated as

$$\hat{\mathbf{e}} = \arg \min_{\mathbf{e}} \left\| \sqrt{\frac{\rho_d}{n}} \hat{\mathbf{A}} \mathbf{e} + \sqrt{\frac{\rho_d}{n}} \Delta \mathbf{x}_0 - \mathbf{w} \right\|^2 + \lambda \rho_d \|\mathbf{e} + \mathbf{x}_0\|^2. \quad (30)$$

Without loss of generality, we assume that

$$\mathbf{x}_0 = \mathbf{1}_n = [1, 1, \dots, 1]^T. \quad (31)$$

Then,

$$\text{BER} = \frac{1}{n} \sum_{i=1}^n \mathbf{1}_{\{\hat{e}_i \leq -1\}}. \quad (32)$$

Next, we note that $\hat{\mathbf{A}}$ can be written as $\hat{\mathbf{A}} = \mathbf{R}_{\hat{\mathbf{A}}}^{1/2} \mathbf{B}$, with \mathbf{B} being a Gaussian matrix with i.i.d. standard entries (0-mean and unit-variance) and $\mathbf{R}_{\hat{\mathbf{A}}}$ is the covariance matrix of $\hat{\mathbf{A}}$ as defined before. Thus, we have

$$\hat{\mathbf{e}} = \arg \min_{\mathbf{e}} \left\| \sqrt{\frac{\rho_d}{n}} \mathbf{R}_{\hat{\mathbf{A}}}^{1/2} \mathbf{B} \mathbf{e} + \sqrt{\frac{\rho_d}{n}} \Delta \mathbf{x}_0 - \mathbf{w} \right\|^2 + \lambda \rho_d \|\mathbf{e} + \mathbf{x}_0\|^2, \quad (33)$$

Since the Gaussian distribution is invariant under orthogonal transformations, and recalling that the spectral decomposition of $\mathbf{R}_{\hat{\mathbf{A}}}$ is $\mathbf{R}_{\hat{\mathbf{A}}} = \mathbf{U} \mathbf{U}^T$, we have

$$\hat{\mathbf{e}} = \arg \min_{\mathbf{e}} \left\| \sqrt{\frac{\rho_d}{n}} \mathbf{\Gamma}^{1/2} \mathbf{B} \mathbf{e} + \sqrt{\frac{\rho_d}{n}} \Delta \mathbf{x}_0 - \mathbf{w} \right\|^2 + \lambda \rho_d \|\mathbf{x}_0 + \mathbf{e}\|^2, \quad (34)$$

with abuse of notation for \mathbf{B} .³ The loss function can be expressed in its dual form through the Fenchel-Legendre conjugate as

$$\begin{aligned} & \left\| \sqrt{\frac{\rho_d}{n}} \mathbf{\Gamma}^{1/2} \mathbf{B} \mathbf{e} + \sqrt{\frac{\rho_d}{n}} \Delta \mathbf{x}_0 - \mathbf{w} \right\|^2 = \\ & \max_{\tilde{\mathbf{u}}} \tilde{\mathbf{u}}^T \left(\sqrt{\frac{\rho_d}{n}} \mathbf{\Gamma}^{1/2} \mathbf{B} \mathbf{e} + \sqrt{\frac{\rho_d}{n}} \Delta \mathbf{x}_0 - \mathbf{w} \right) - \frac{\|\tilde{\mathbf{u}}\|^2}{4}. \end{aligned}$$

Then, (34) becomes

$$\begin{aligned} \Phi^{(n)} := & \min_{\mathbf{e}} \max_{\tilde{\mathbf{u}}} \sqrt{\frac{\rho_d}{n}} \tilde{\mathbf{u}}^T \mathbf{\Gamma}^{1/2} \mathbf{B} \mathbf{e} + \sqrt{\frac{\rho_d}{n}} \tilde{\mathbf{u}}^T \Delta \mathbf{x}_0 \\ & - \tilde{\mathbf{u}}^T \mathbf{w} - \frac{\|\tilde{\mathbf{u}}\|^2}{4} + \lambda \rho_d \|\mathbf{x}_0 + \mathbf{e}\|^2. \end{aligned} \quad (35)$$

One technical requirement of the cGMT is the compactness of the feasibility sets. This can be handled according to the approach in [22, Appendix A], by introducing sufficiently large *artificial* constraint sets $\mathcal{K}_{\mathbf{e}} = \{\mathbf{e} \in \mathbb{R}^n : \|\mathbf{e}\|_2 \leq C_e\}$, and $\mathcal{K}_{\tilde{\mathbf{u}}} = \{\tilde{\mathbf{u}} \in \mathbb{R}^m : \|\tilde{\mathbf{u}}\|_2 \leq C_{\tilde{\mathbf{u}}}\}$ for some sufficiently large constants (independent of n) $C_e, C_{\tilde{\mathbf{u}}} > 0$, which will not asymptotically affect the optimisation problem. Then, we obtain

$$\begin{aligned} \tilde{\Phi}^{(n)} = & \min_{\mathbf{e} \in \mathcal{K}_{\mathbf{e}}} \max_{\tilde{\mathbf{u}} \in \mathcal{K}_{\tilde{\mathbf{u}}}} \sqrt{\frac{\rho_d}{n}} \tilde{\mathbf{u}}^T \mathbf{\Gamma}^{1/2} \mathbf{B} \mathbf{e} + \sqrt{\frac{\rho_d}{n}} \tilde{\mathbf{u}}^T \Delta \mathbf{x}_0 \\ & - \tilde{\mathbf{u}}^T \mathbf{w} - \frac{\|\tilde{\mathbf{u}}\|^2}{4} + \lambda \rho_d \|\mathbf{x}_0 + \mathbf{e}\|^2. \end{aligned} \quad (36)$$

³We reused \mathbf{B} to denote another standard Gaussian matrix.

The above optimisation problem is now in the desired min-max form of a PO problem of the cGMT. However, we still have correlated entries in the bi-linear term and we have to transform them to a term that involves a standard Gaussian matrix with i.i.d. entries (as required by the cGMT statement). To do so, redefine $\tilde{\mathbf{u}} = \mathbf{\Gamma}^{1/2} \tilde{\mathbf{u}}$. Then, after properly normalising $\tilde{\Phi}^{(n)}$ by $\frac{1}{n}$, it becomes

$$\begin{aligned} \bar{\Phi}^{(n)} = & \frac{1}{\sqrt{n}} \left[\min_{\mathbf{e} \in \mathcal{K}_{\mathbf{e}}} \max_{\tilde{\mathbf{u}} \in \mathcal{K}_{\tilde{\mathbf{u}}}} \frac{\sqrt{\rho_d}}{n} \tilde{\mathbf{u}}^T \mathbf{B} \mathbf{e} + \frac{\sqrt{\rho_d}}{n} \tilde{\mathbf{u}}^T \mathbf{\Gamma}^{-1/2} \Delta \mathbf{x}_0 \right. \\ & \left. - \frac{1}{\sqrt{n}} \tilde{\mathbf{u}}^T \mathbf{\Gamma}^{-1/2} \mathbf{w} - \frac{\tilde{\mathbf{u}}^T \mathbf{\Gamma}^{-1} \tilde{\mathbf{u}}}{4\sqrt{n}} + \frac{\lambda \rho_d}{\sqrt{n}} \|\mathbf{x}_0 + \mathbf{e}\|^2 \right]. \end{aligned} \quad (37)$$

The above optimisation is in a PO form, and its corresponding AO is

$$\begin{aligned} \phi^{(n)} := & \frac{1}{\sqrt{n}} \left[\min_{\mathbf{e} \in \mathcal{K}_{\mathbf{e}}} \max_{\tilde{\mathbf{u}} \in \mathcal{K}_{\tilde{\mathbf{u}}}} \frac{\sqrt{\rho_d}}{n} \|\mathbf{e}\| \mathbf{g}^T \tilde{\mathbf{u}} - \frac{\sqrt{\rho_d}}{n} \|\tilde{\mathbf{u}}\| \mathbf{s}^T \mathbf{e} \right. \\ & + \frac{\sqrt{\rho_d}}{n} \tilde{\mathbf{u}}^T \mathbf{\Gamma}^{-1/2} \Delta \mathbf{x}_0 - \frac{1}{\sqrt{n}} \tilde{\mathbf{u}}^T \mathbf{\Gamma}^{-1/2} \mathbf{w} \\ & \left. - \frac{\tilde{\mathbf{u}}^T \mathbf{\Gamma}^{-1} \tilde{\mathbf{u}}}{4\sqrt{n}} + \frac{\lambda \rho_d}{\sqrt{n}} \|\mathbf{x}_0 + \mathbf{e}\|^2 \right], \end{aligned} \quad (38)$$

where $\mathbf{g} \in \mathbb{R}^m$ and $\mathbf{s} \in \mathbb{R}^n$ are independent random vectors with i.i.d. standard normal entries each.

Fixing the norm of the normalised error vector, $\frac{\|\mathbf{e}\|}{\sqrt{n}}$, to $\eta := \frac{\|\mathbf{e}\|}{\sqrt{n}}$, and defining $\bar{\mathbf{e}} := \frac{\mathbf{e}}{\|\mathbf{e}\|}$ yields

$$\begin{aligned} \phi^{(n)} = & \min_{\eta > 0} \min_{\|\bar{\mathbf{e}}\|=1} \max_{\tilde{\mathbf{u}} \in \mathcal{K}_{\tilde{\mathbf{u}}}} \frac{\eta \sqrt{\rho_d}}{n} \mathbf{g}^T \tilde{\mathbf{u}} - \frac{\eta \sqrt{\rho_d}}{n} \|\tilde{\mathbf{u}}\| \mathbf{s}^T \bar{\mathbf{e}} \\ & + \frac{\sqrt{\rho_d}}{n \sqrt{n}} \tilde{\mathbf{u}}^T \mathbf{\Gamma}^{-1/2} \Delta \mathbf{x}_0 - \frac{1}{n} \tilde{\mathbf{u}}^T \mathbf{\Gamma}^{-1/2} \mathbf{w} - \frac{1}{4n} \tilde{\mathbf{u}}^T \mathbf{\Gamma}^{-1} \tilde{\mathbf{u}} \\ & + \lambda \rho_d \eta^2 + \frac{2\lambda \rho_d \eta}{\sqrt{n}} \mathbf{x}_0^T \bar{\mathbf{e}} + \frac{\lambda \rho_d}{n} \|\mathbf{x}_0\|^2. \end{aligned} \quad (39)$$

Defining $\mathbf{u} := \frac{\tilde{\mathbf{u}}}{\sqrt{n}}$ gives:

$$\begin{aligned} \phi^{(n)} = & \min_{\eta > 0} \max_{\mathbf{u} \in \mathcal{K}_{\mathbf{u}}} \frac{\eta \sqrt{\rho_d}}{\sqrt{n}} \mathbf{g}^T \mathbf{u} + \frac{\sqrt{\rho_d}}{n} \mathbf{u}^T \mathbf{\Gamma}^{-1/2} \Delta \mathbf{x}_0 \\ & - \frac{1}{\sqrt{n}} \mathbf{u}^T \mathbf{\Gamma}^{-1/2} \mathbf{w} - \frac{1}{4} \mathbf{u}^T \mathbf{\Gamma}^{-1} \mathbf{u} + \lambda \rho_d \eta^2 \\ & + \frac{\lambda \rho_d}{n} \|\mathbf{x}_0\|^2 + \min_{\|\bar{\mathbf{e}}\|=1} \frac{\eta}{\sqrt{n}} (2\lambda \rho_d \mathbf{x}_0 - \sqrt{\rho_d} \|\mathbf{u}\| \mathbf{s})^T \bar{\mathbf{e}}, \end{aligned} \quad (40)$$

where $\mathcal{K}_{\mathbf{u}}$ is defined in a similar fashion to $\mathcal{K}_{\tilde{\mathbf{u}}}$. The optimisation over $\bar{\mathbf{e}}$ can be easily found as follows

$$\begin{aligned} & \min_{\|\bar{\mathbf{e}}\|=1} \frac{\eta}{\sqrt{n}} \left(2\lambda \rho_d \mathbf{x}_0 - \sqrt{\rho_d} \|\mathbf{u}\| \mathbf{s} \right)^T \bar{\mathbf{e}} \\ & = -\frac{\eta}{\sqrt{n}} \left\| 2\lambda \rho_d \mathbf{x}_0 - \sqrt{\rho_d} \|\mathbf{u}\| \mathbf{s} \right\| \\ & \xrightarrow{P} -\eta \sqrt{4\lambda^2 \rho_d^2 + \rho_d \|\mathbf{u}\|^2}, \end{aligned} \quad (41)$$

with a minimiser:

$$\bar{\mathbf{e}} = -\frac{2\lambda \rho_d \mathbf{x}_0 - \sqrt{\rho_d} \|\mathbf{u}\|_2 \mathbf{s}}{\left\| 2\lambda \rho_d \mathbf{x}_0 - \sqrt{\rho_d} \|\mathbf{u}\|_2 \mathbf{s} \right\|}. \quad (42)$$

Also, note that $\frac{1}{n}\|\mathbf{x}_0\|^2 \xrightarrow{P} 1$. Thus, by applying Lemma 10 in [22], we have

$$\tilde{\phi}^{(n)} - \phi^{(n)} \xrightarrow{P} 0, \quad (43)$$

where

$$\begin{aligned} \tilde{\phi}^{(n)} = & \min_{\eta>0} \max_{\mathbf{u} \in \mathcal{K}_{\mathbf{u}}} \frac{1}{\sqrt{n}} \left(\eta \sqrt{\rho_d} \mathbf{g} + \sqrt{\frac{\rho_d}{n}} \mathbf{\Gamma}^{-1/2} \mathbf{\Delta} \mathbf{x}_0 - \mathbf{\Gamma}^{-1/2} \mathbf{w} \right)^T \mathbf{u} \\ & - \frac{1}{4} \mathbf{u}^T \mathbf{\Gamma}^{-1} \mathbf{u} + \lambda \rho_d (\eta^2 + 1) - \eta \sqrt{4\lambda^2 \rho_d^2 + \rho_d \|\mathbf{u}\|^2}. \end{aligned} \quad (44)$$

The square root in the last term of the above equation can be written in a variational form using the following identity

$$\Theta = \min_{\chi>0} \frac{\chi}{2} + \frac{\Theta^2}{2\chi}, \quad (45)$$

with $\Theta = \sqrt{4\lambda^2 \rho_d^2 + \rho_d \|\mathbf{u}\|^2}$. Hence, $\tilde{\phi}^{(n)}$ becomes

$$\begin{aligned} \tilde{\phi}^{(n)} = & \min_{\eta>0} \max_{\substack{\mathbf{u} \in \mathcal{K}_{\mathbf{u}} \\ \chi>0}} \left(\eta \sqrt{\rho_d} \mathbf{g} + \sqrt{\frac{\rho_d}{n}} \mathbf{\Gamma}^{-1/2} \mathbf{\Delta} \mathbf{x}_0 - \mathbf{\Gamma}^{-1/2} \mathbf{w} \right)^T \frac{\mathbf{u}}{\sqrt{n}} \\ & - \frac{1}{4} \mathbf{u}^T \mathbf{\Gamma}^{-1} \mathbf{u} + \lambda \rho_d (\eta^2 + 1) - \frac{\eta \chi}{2} - \frac{\eta (4\lambda^2 \rho_d^2 + \rho_d \|\mathbf{u}\|^2)}{2\chi}. \end{aligned} \quad (46)$$

Next, for convenience, let

$$\tilde{\mathbf{g}} := \eta \sqrt{\rho_d} \mathbf{g} + \sqrt{\frac{\rho_d}{n}} \mathbf{\Gamma}^{-1/2} \mathbf{\Delta} \mathbf{x}_0 - \mathbf{\Gamma}^{-1/2} \mathbf{w}, \quad (47)$$

and

$$\mathbf{T} := \frac{1}{2} \mathbf{\Gamma}^{-1} + \frac{\rho_d \eta}{\chi} \mathbf{I}_m, \quad (48)$$

then,

$$\begin{aligned} \tilde{\phi}^{(n)} = & \min_{\eta>0} \max_{\substack{\mathbf{u} \in \mathcal{K}_{\mathbf{u}} \\ \chi>0}} \frac{1}{\sqrt{n}} \tilde{\mathbf{g}}^T \mathbf{u} - \frac{1}{2} \mathbf{u}^T \mathbf{T} \mathbf{u} \\ & - \frac{\eta \chi}{2} - \frac{2\lambda^2 \rho_d^2 \eta}{\chi} + \lambda \rho_d (\eta^2 + 1). \end{aligned} \quad (49)$$

The optimisation over \mathbf{u} is straightforward:

$$\mathbf{u}_* = \frac{1}{\sqrt{n}} \mathbf{T}^{-1} \tilde{\mathbf{g}}. \quad (50)$$

Then, the AO writes

$$\begin{aligned} \tilde{\phi}^{(n)} = & \min_{\eta>0} \max_{\chi>0} \frac{1}{2n} \tilde{\mathbf{g}}^T \mathbf{T}^{-1} \tilde{\mathbf{g}} - \frac{\eta \chi}{2} \\ & - \frac{2\lambda^2 \rho_d^2 \eta}{\chi} + \lambda \rho_d (\eta^2 + 1). \end{aligned} \quad (51)$$

The above optimisation is now over scalar variables only, namely η and χ which is easier to analyse. We will refer to (51) as the *Scalar Optimisation Problem* (SOP) and study its asymptotic behaviour next.

C. Analysis of the Asymptotic Behaviour of the SOP

First, note that $\tilde{\mathbf{g}} \sim \mathcal{N}(\mathbf{0}, \mathbf{R}_{\tilde{\mathbf{g}}})$, where⁴

$$\mathbf{R}_{\tilde{\mathbf{g}}} = \rho_d \eta^2 \mathbf{I}_m + (\rho_d \mathbf{R}_{\Delta} + \mathbf{I}_m) \mathbf{\Gamma}^{-1}. \quad (52)$$

Then, using tools from random matrix theory (RMT) such as the Trace Lemma [36], we have

$$\frac{1}{n} \tilde{\mathbf{g}}^T \mathbf{T}^{-1} \tilde{\mathbf{g}} - \frac{1}{n} \text{tr}(\mathbf{R}_{\tilde{\mathbf{g}}} \mathbf{T}^{-1}) \xrightarrow{P} 0. \quad (53)$$

Therefore, again, using [22, Lemma 10], $\tilde{\phi}^{(n)} - \bar{\phi}^{(n)} \xrightarrow{P} 0$, where

$$\begin{aligned} \bar{\phi}^{(n)} := & \min_{\eta>0} \max_{\chi>0} \frac{1}{2n} \sum_{j=1}^m \frac{\gamma_j \rho_d \eta^2 + 1 + \rho_d [\mathbf{R}_{\Delta}]_{jj}}{\frac{1}{2} + \frac{\eta \rho_d \gamma_j}{\chi}} \\ & + \lambda \rho_d (\eta^2 + 1) - \frac{\eta \chi}{2} - \frac{2\lambda^2 \rho_d^2 \eta}{\chi}. \end{aligned} \quad (54)$$

Defining $\mu := \frac{\chi}{\eta}$, we get

$$\begin{aligned} \bar{\phi}^{(n)} = & \min_{\eta>0} \max_{\mu>0} \frac{1}{2n} \sum_{j=1}^m \frac{\gamma_j \rho_d \eta^2 + \rho_d [\mathbf{R}_{\Delta}]_{jj} + 1}{\frac{1}{2} + \frac{\rho_d \gamma_j}{\mu}} \\ & + \lambda \rho_d (\eta^2 + 1) - \frac{\eta^2 \mu}{2} - \frac{2\lambda^2 \rho_d^2}{\mu}. \end{aligned} \quad (55)$$

Finally, note that η appears everywhere in $\bar{\phi}^{(n)}$ as η^2 , so we can use the change of variable $\nu := \eta^2$ to have

$$\begin{aligned} \bar{\phi}^{(n)} = & \min_{\nu>0} \max_{\mu>0} \frac{1}{2n} \sum_{j=1}^m \frac{\gamma_j \rho_d \nu + \rho_d [\mathbf{R}_{\Delta}]_{jj} + 1}{\frac{1}{2} + \frac{\rho_d \gamma_j}{\mu}} \\ & + \lambda \rho_d (\nu + 1) - \frac{\nu \mu}{2} - \frac{2\lambda^2 \rho_d^2}{\mu}. \end{aligned} \quad (56)$$

D. Exact Asymptotics of RZF via the cGMT

We are now in a position to study the asymptotic behaviour of the RZF receiver.

MSE Analysis: Let $\tilde{\mathbf{e}}$ be the optimal solution to the AO defined as the solution to (40). Let ν_* be the optimal solution to (56). For any $\epsilon > 0$, define the set:

$$\mathcal{K}_{\epsilon} = \left\{ \mathbf{v} : \left| \frac{1}{n} \|\mathbf{v}\|^2 - \nu_* \right| < \epsilon \right\}. \quad (57)$$

Denote $\hat{\eta}$ as a minimiser of (55). By definition, $\hat{\eta} = \frac{\|\tilde{\mathbf{e}}\|}{n}$, or using the change of variables that we introduced, $\hat{\nu} = \frac{\|\tilde{\mathbf{e}}\|^2}{n}$. We have shown in the previous section that $\phi^{(n)} - \bar{\phi}^{(n)} \xrightarrow{P} 0$, and since $\bar{\phi}^{(n)}$ in (56) has a unique minimiser ν_* , then, applying Lemma 10 in [22]: $\hat{\nu} - \nu_* \xrightarrow{P} 0$, which implies that

$$\left| \frac{1}{n} \|\tilde{\mathbf{e}}\|^2 - \nu_* \right| \xrightarrow{P} 0. \quad (58)$$

This proves that $\tilde{\mathbf{e}} \in \mathcal{K}_{\epsilon}$ with probability approaching 1. Then, applying the cGMT yields that $\hat{\mathbf{e}} \in \mathcal{K}_{\epsilon}$ with probability approaching 1 as well. This completes the proof of Theorem 1.

⁴This result is based on the assumption that $\mathbf{x}_0 = \mathbf{1}_n$.

BER Analysis: For the BER analysis, we will change the set \mathcal{K}_ϵ in (57) to the following:

$$\mathcal{K}_\epsilon = \left\{ \mathbf{v} : \left| \frac{1}{n} \sum_{i=1}^n \mathbf{1}_{\{v_i \leq -1\}} - Q \left(\sqrt{\frac{4\lambda^2 \rho_d (1 - \nu_*) + F_\gamma(\nu_*, \mu_*)}{\nu_* F_\gamma(\nu_*, \mu_*)}} \right) \right| < \epsilon \right\}.$$

Recall that the optimal solution of the AO in (42) is given as:

$$\tilde{\mathbf{e}} = -\hat{\gamma} \sqrt{n} \frac{2\gamma \mathbf{x}_0 - \|\mathbf{u}_*\| \mathbf{s}}{\|2\gamma \mathbf{x}_0 - \|\mathbf{u}_*\| \mathbf{s}\|}. \quad (59)$$

Also, remember that $\mathbf{u}_* = \frac{1}{\sqrt{n}} \mathbf{T}^{-1} \tilde{\mathbf{g}}$, then, $\|\mathbf{u}_*\|^2 = \frac{1}{n} \tilde{\mathbf{g}}^T \mathbf{T}^{-2} \tilde{\mathbf{g}}^T$. Then, using the Trace Lemma, we have

$$\frac{1}{n} \tilde{\mathbf{g}}^T \mathbf{T}^{-2} \tilde{\mathbf{g}}^T - \frac{1}{n} \text{tr}(\mathbf{R}_{\tilde{\mathbf{g}}} \mathbf{T}^{-2}) \xrightarrow{P} 0. \quad (60)$$

Or, define

$$S_\gamma(\nu, \mu) := \frac{1}{n} \text{tr}(\mathbf{R}_{\tilde{\mathbf{g}}} \mathbf{T}^{-2}) = \frac{1}{n} \sum_{j=1}^m \frac{\rho_d \gamma_j^2 \nu + \rho_d \gamma_j (\rho_d [\mathbf{R}_\Delta]_{jj} + 1)}{\left(\frac{1}{2} + \frac{\rho_d \gamma_j}{\mu}\right)^2},$$

then,

$$\|\mathbf{u}_*\|_2^2 - S_\gamma(\hat{\nu}, \hat{\mu}) \xrightarrow{P} 0. \quad (61)$$

Using the fact that $\hat{\nu} - \nu_* \xrightarrow{P} 0$ and $\hat{\mu} - \mu_* \xrightarrow{P} 0$, then for all $i = 1, 2, \dots, n$, we have

$$\left| \tilde{e}_i - \frac{-\sqrt{\nu_*} \left(2\rho_d \lambda - \sqrt{\rho_d S_\gamma(\nu_*, \mu_*)} s_i \right)}{\sqrt{4\rho_d^2 \lambda^2 + \rho_d S_\gamma(\nu_*, \mu_*)}} \right| \xrightarrow{P} 0. \quad (62)$$

Hence, using the above expression of $\tilde{\mathbf{e}}$, we have

$$\begin{aligned} & \frac{1}{n} \sum_{i=1}^n \mathbf{1}_{\{\tilde{e}_i \leq -1\}} \\ &= \frac{1}{n} \sum_{i=1}^n \mathbf{1}_{\left\{ s_i \leq \frac{2\lambda \sqrt{\rho_d \nu_*} - \sqrt{4\rho_d^2 \lambda^2 + \rho_d S_\gamma(\nu_*, \mu_*)}}{\sqrt{\nu_* S_\gamma(\nu_*, \mu_*)}} \right\}}, \end{aligned} \quad (63)$$

from which we can easily get

$$\left| \frac{1}{n} \sum_{i=1}^n \mathbf{1}_{\{\tilde{e}_i \leq -1\}} - Q \left(\sqrt{\frac{4\lambda^2 \rho_d (1 - \nu_*) + S_\gamma(\nu_*, \mu_*)}{\nu_* S_\gamma(\nu_*, \mu_*)}} \right) \right| \xrightarrow{P} 0.$$

Therefore, $\tilde{\mathbf{e}} \in \mathcal{K}_\epsilon$ with probability approaching one. Note that the indicator function $\mathbf{1}_{\{\tilde{e}_i \leq -1\}}$ is not Lipschitz, so we cannot directly apply the cGMT. However, as discussed in [23, Lemma A.4], this function can be appropriately approximated with Lipschitz functions. Therefore, we can conclude by applying the cGMT that $\hat{\mathbf{e}} \in \mathcal{K}_\epsilon$ with probability approaching one, which proves Theorem 2.

REFERENCES

- [1] Thomas L Marzetta, "Noncooperative cellular wireless with unlimited numbers of base station antennas," *IEEE transactions on wireless communications*, vol. 9, no. 11, pp. 3590–3600, 2010.
- [2] Erik G Larsson, Ove Edfors, Fredrik Tufvesson, and Thomas L Marzetta, "Massive mimo for next generation wireless systems," *IEEE communications magazine*, vol. 52, no. 2, pp. 186–195, 2014.
- [3] Emil Björnson, Jakob Hoydis, and Luca Sanguinetti, *Massive MIMO networks: Spectral, energy, and hardware efficiency*, Now Publishers Inc. Hanover, MA, USA, 2017.
- [4] Tarig Ballal, Mohamed A Suliman, Ayed M Alrashdi, and Tareq Y Al-Naffouri, "Optimum pilot and data energy allocation for bpsk transmission over massive mimo systems," in *2019 IEEE Wireless Communications and Networking Conference (WCNC)*. IEEE, 2019, pp. 1–6.
- [5] Peiyue Zhao, Gábor Fodor, György Dán, and Miklós Telek, "A game theoretic approach to setting the pilot power ratio in multi-user mimo systems," *IEEE Transactions on Communications*, vol. 66, no. 3, pp. 999–1012, 2017.
- [6] Kezhi Wang, Yunfei Chen, Mohamed-Slim Alouini, and Feng Xu, "Ber and optimal power allocation for amplify-and-forward relaying using pilot-aided maximum likelihood estimation," *IEEE Transactions on Communications*, vol. 62, no. 10, pp. 3462–3475, 2014.
- [7] Ayed Alrashdi, Abla Kammoun, Ali H Muqabail, and Tareq Y Al-Naffouri, "Optimum m-pam transmission for massive mimo systems with channel uncertainty," *arXiv preprint arXiv:2008.06993*, 2020.
- [8] Ayed M Alrashdi, Ismail Ben Atitallah, Tarig Ballal, Christos Thrampoulidis, Anas Chaaban, and Tareq Y Al-Naffouri, "Optimum training for mimo bpsk transmission," in *2018 IEEE 19th International Workshop on Signal Processing Advances in Wireless Communications (SPAWC)*. IEEE, 2018, pp. 1–5.
- [9] VK Varma Gottumukkala and Hlaing Minn, "Optimal pilot power allocation for ofdm systems with transmitter and receiver iq imbalances," in *GLOBECOM 2009-2009 IEEE Global Telecommunications Conference*. IEEE, 2009, pp. 1–5.
- [10] Arun P Kannu and Philip Schniter, "Capacity analysis of mmse pilot-aided transmission for doubly selective channels," in *IEEE 6th Workshop on Signal Processing Advances in Wireless Communications*, 2005. IEEE, 2005, pp. 801–805.
- [11] Babak Hassibi and Bertrand M Hochwald, "How much training is needed in multiple-antenna wireless links?," *IEEE Transactions on Information Theory*, vol. 49, no. 4, pp. 951–963, 2003.
- [12] Hieu Trong Dao and Sunghwan Kim, "Pilot power allocation for maximizing the sum rate in massive mimo systems," *IET Communications*, vol. 12, no. 11, pp. 1367–1372, 2018.
- [13] Yasong Zhu, Hairong Wang, and Chen Liu, "Uplink pilot-to-data power ratio design based on user joint optimization algorithm in multi-cell massive mimo system," in *2018 IEEE 18th International Conference on Communication Technology (ICCT)*. IEEE, 2018, pp. 396–401.
- [14] Songtao Lu and Zhengdao Wang, "Training optimization and performance of single cell uplink system with massive-antennas base station," *IEEE Transactions on Communications*, vol. 67, no. 2, pp. 1570–1585, 2018.
- [15] Hei Victor Cheng, Emil Björnson, and Erik G Larsson, "Optimal pilot and payload power control in single-cell massive mimo systems," *IEEE Transactions on Signal Processing*, vol. 65, no. 9, pp. 2363–2378, 2016.
- [16] Pei Liu, Shi Jin, Tao Jiang, Qi Zhang, and Michail Matthaiou, "Pilot power allocation through user grouping in multi-cell massive mimo systems," *Ieee transactions on communications*, vol. 65, no. 4, pp. 1561–1574, 2016.
- [17] Trinh Van Chien, Emil Björnson, and Erik G Larsson, "Joint pilot design and uplink power allocation in multi-cell massive mimo systems," *IEEE Transactions on Wireless Communications*, vol. 17, no. 3, pp. 2000–2015, 2018.
- [18] Emil Björnson, Jakob Hoydis, and Luca Sanguinetti, "Massive mimo networks: Spectral, energy, and hardware efficiency," *Foundations and Trends in Signal Processing*, vol. 11, no. 3-4, pp. 154–655, 2017.
- [19] Sebastian Wagner, Romain Couillet, Mérouane Debbah, and Dirk TM Slock, "Large system analysis of linear precoding in correlated miso broadcast channels under limited feedback," *IEEE transactions on information theory*, vol. 58, no. 7, pp. 4509–4537, 2012.
- [20] Rusdha Muharar, "Optimal power allocation and training duration for uplink multiuser massive mimo systems with mmse receivers," *IEEE Access*, vol. 8, pp. 23378–23390, 2020.
- [21] Ikram Boukhedimi, Abla Kammoun, and Mohamed-Slim Alouini, "Lmmse receivers in uplink massive mimo systems with correlated rician fading," *IEEE Transactions on Communications*, vol. 67, no. 1, pp. 230–243, 2018.
- [22] Christos Thrampoulidis, Ehsan Abbasi, and Babak Hassibi, "Precise error analysis of regularized m -estimators in high dimensions," *IEEE Transactions on Information Theory*, vol. 64, no. 8, pp. 5592–5628, 2018.
- [23] Christos Thrampoulidis, Weiye Xu, and Babak Hassibi, "Symbol error rate performance of box-relaxation decoders in massive mimo," *IEEE Transactions on Signal Processing*, vol. 66, no. 13, pp. 3377–3392, 2018.
- [24] Ayed M Alrashdi, Ismail Ben Atitallah, Tareq Y Al-Naffouri, and Mohamed-Slim Alouini, "Precise performance analysis of the lasso

- under matrix uncertainties,” in *2017 IEEE Global Conference on Signal and Information Processing (GlobalSIP)*. IEEE, 2017, pp. 1290–1294.
- [25] Ismail Ben Atitallah, Christos Thrampoulidis, Abba Kammoun, Tareq Y Al-Naffouri, Mohamed-Slim Alouini, and Babak Hassibi, “The box-lasso with application to gsk modulation in massive mimo systems,” in *2017 IEEE International Symposium on Information Theory (ISIT)*. IEEE, 2017, pp. 1082–1086.
- [26] Ayed M Alrashdi, Ismail Ben Atitallah, and Tareq Y Al-Naffouri, “Precise performance analysis of the box-elastic net under matrix uncertainties,” *IEEE Signal Processing Letters*, vol. 26, no. 5, pp. 655–659, 2019.
- [27] Oussama Dhifallah and Yue M Lu, “A precise performance analysis of learning with random features,” *arXiv preprint arXiv:2008.11904*, 2020.
- [28] Ryo Hayakawa and Kazunori Hayashi, “Asymptotic performance of discrete-valued vector reconstruction via box-constrained optimization with sum of ℓ_1 regularizers,” *IEEE Transactions on Signal Processing*, vol. 68, pp. 4320–4335, 2020.
- [29] Ayed M Alrashdi, Housseem Sifaou, Abba Kammoun, Mohamed-Slim Alouini, and Tareq Y Al-Naffouri, “Box-relaxation for bpsk recovery in massive mimo: A precise analysis under correlated channels,” in *ICC 2020-2020 IEEE International Conference on Communications (ICC)*. IEEE, 2020, pp. 1–6.
- [30] Ayed M Alrashdi, Housseem Sifaou, Abba Kammoun, Mohamed-Slim Alouini, and Tareq Y Al-Naffouri, “Precise error analysis of the lasso under correlated designs,” *arXiv preprint arXiv:2008.13033*, 2020.
- [31] Sebastian Wagner, Romain Couillet, Mérouane Debbah, and Dirk T. M. Slock, “Large system analysis of linear precoding in correlated mimo broadcast channels under limited feedback,” *IEEE Transactions on Information Theory*, vol. 58, no. 7, pp. 4509–4537, 2012.
- [32] Steven M Kay, *Fundamentals of statistical signal processing*, Prentice Hall PTR, 1993.
- [33] Jakob Hoydis, Stephan Ten Brink, and Mérouane Debbah, “Massive mimo in the ul/dl of cellular networks: How many antennas do we need?,” *IEEE Journal on selected Areas in Communications*, vol. 31, no. 2, pp. 160–171, 2013.
- [34] Christian B Peel, Bertrand M Hochwald, and A Lee Swindlehurst, “A vector-perturbation technique for near-capacity multiantenna multiuser communication-part i: channel inversion and regularization,” *IEEE Transactions on Communications*, vol. 53, no. 1, pp. 195–202, 2005.
- [35] Giuseppa Alfano, Antonia M Tulino, Angel Lozano, and Sergio Verdú, “Capacity of mimo channels with one-sided correlation,” in *Eighth IEEE International Symposium on Spread Spectrum Techniques and Applications-Programme and Book of Abstracts (IEEE Cat. No. 04TH8738)*. IEEE, 2004, pp. 515–519.
- [36] T. Couillet and M. Debbah, *Random Matrix Methods for Wireless Communications*, U.K., Cambridge: Cambridge Univ. Press, 2011.



Ayed M. Alrashdi received the B.S. degree in Electrical Engineering (with first honors) from University of Hail, Hail, Saudi Arabia, in 2014, and the M.S. degree in Electrical Engineering from King Abdullah University of Science and Technology (KAUST), Thuwal, Saudi Arabia, in 2016. He received the Ph.D. degree in Electrical and Computer Engineering from KAUST in 2021.

From 2017 to 2021, he was a Research Assistant with the Information System Lab (ISL) at KAUST. Currently, he is an assistant professor in the Electrical Engineering Department at University of Ha'il, Saudi Arabia. His research interests are in the areas of statistical signal processing, high-dimensional statistics, compressed sensing, statistical learning, and wireless communications.